Desalination and Water Treatment
www.deswater.com
doi: 10.5004/dwt.2020.25620

190 (2020) 147–155
June

Photocatalytic degradation of bisphenol-A in aqueous solution by calcined PbO semiconductor irradiated with visible light

Wen-Shing Chen*, Shih-Lun Huang

Department of Chemical and Materials Engineering, National Yunlin University of Science & Technology, 123 University Road, Section 3, Douliou, Yunlin 640, Taiwan, Tel. +886-5-534-2601 Ext: 4624; Fax: +886-5-531-2071; email: chenwen@yuntech.edu.tw (W.-S. Chen)

Received 6 September 2019; Accepted 24 January 2020

ABSTRACT

Oxidative degradation of bisphenol-A in aqueous solution was conducted under visible light irradiation using PbO semiconductor, of which band gap energy was reduced from 2.61 to 1.99 eV, caused by smoothening surface morphology via the calcination treatment. The characteristics of original and reacted PbO (calcined) were illustrated by X-ray diffraction patterns, FE-SEM images, Brunauer–Emmett–Teller specific surface areas, UV-Vis diffuse reflectance spectra and X-ray photoelectron spectra respectively. Experiments were carried out in the batch-wise mode to investigate the influence of various operation variables on the photocatalytic behavior, such as temperature, a dosage of PbO and sodium sulfate concentrations. In this study, bisphenol-A could be almost entirely decomposed through PbO coupled with visible light irradiation, wherein photogenerated holes and hydroxyl radicals were presumed to be principal oxidizing agents. Besides, the removal percentage of bisphenol-A was significantly enhanced on the addition of sodium sulfate, in which sulfate anions were transformed into sulfate radicals via photogenerated holes. On the whole, PbO semiconductors integrated with visible light irradiation appear to be an economical and promising method for disposal of wastewater containing bisphenol-A.

Keywords: Bisphenol-A; PbO; Semiconductor; Photocatalysis; Hydroxyl radicals

1. Introduction

Bisphenol-A is an extremely important phenolic compound due to its substantial demand for the synthesis of epoxy resin upon reaction with epichlorohydrin. Besides, polycarbonates could be obtained by condensation of bisphenol-A and phosgene. Bisphenol-A has been also used as precursor for the manufacture of thermoplastic polymers, such as polysulfones [1]. Nonetheless, bisphenol-A has become one of the emergent environmental contaminants, due to its cellular toxicity and severe damage to the endocrine system, and the wastewater effluent polluted by bisphenol-A should be properly disposed [2,3].

In the last decade, the photocatalytic processes have attracted much attention for oxidative degradation of bisphenol-A in wastewater on account of several advantages over other advanced oxidation processes, such as reduction of chemicals used, efficient energy consumption and operation under ambient conditions. TiO_2 has been the most suitable photocatalyst in application to wastewater treatment owing to its high photocatalytic activity, corrosion-resistant, low cost and toxicity. Several publications have been issued on the oxidative degradation of bisphenol-A using TiO_2/UV based techniques. The photogenerated electrons on the surface of TiO_2 are rapidly separated from the holes with the assistance of graphene oxide (GO), wherein the steric structure of photocatalysts facilitates recovery of TiO_2/GO [4]. Kondrakov et al. [5] claim that photogenerated holes are mainly responsible for the degradation of bisphenol-A. The reaction pathway was hypothesized based on

* Corresponding author.

intermediates identified, including catechol, dicatechol and quinone. Additionally, TiO_2 was cooperated with various supports to enhance the photocatalytic activity utilizing increasing active sites and/or organics adsorption capacities, such as glass fiber [6], wood charcoal [7], ceramics [8] and titanate [9]. Another advantage provided from the supports was to make photocatalysts easily separated from the aqueous solution. Alternatively, some researchers promoted the separation of photogenerated electrons and holes on the TiO_2, leading to significant enhancement on the amounts of hydroxyl radicals, through the synthesis of TiO_2-SnO_2 [10], TiO_2-MoS_2 [11] and TiO_2-Gd_2O_3 [12] composites respectively, wherein the kinetic model for the degradation of bisphenol-A was described by the pseudo-first-order rate equation.

Recently, tremendous efforts have been carried out to modify TiO_2 so that it can be photoresponsive to visible light irradiation for the sake of harnessing the major domains of the solar spectrum. Yap et al. [13,14] doped nitrogen atom from urea into TiO_2 crystallites interstice successfully and extended the absorption band of TiO_2 to the visible light region. The photogenerated holes played dominant roles for the removal of bisphenol-A, of which degradation rate decreased significantly in the presence of inorganic anions (Cl^-, NO_3^-, HCO_3^-) and organic anion ($C_2O_4^{2-}$) individually. On the other hand, TiO_2 was responsive to visible light irradiation effectively by co-doping with carbon-nitrogen elements, wherein nitrogen defects promote separation of photogenerated charges and induce reactive oxygen species [15,16]. Besides, metal oxides have been used as dopants, including Cu_2O [17], CuO [18], PrO_2 [19], WO_3 [20] and ZnO [21]. The metal ions served as an electron sink and reinforced charge separation, leading to inhibition of the recombination of photogenerated electrons with holes on the surface of TiO_2 and the promotion of photocatalytic ability [22,23]. Furthermore, Nguyen et al. [24] fabricated a composite photocatalyst, coupling p-type $ZnFe_2O_4$ with *n*-type TiO_2 semiconductors, for photocatalytic oxidation of bisphenol-A. The photogenerated holes and hydroxyl radicals were considered to be the main oxidants.

It has been recognized that at the near-UV light (λ < 400 nm) domain TiO_2 is photosensitive, of which band gap energy is about 3.2 eV. To tune the light absorption band of TiO_2 into a visible light range, some researchers have also focused on PbO as the promoter [25,26]. It has been well known that PbO is a widely used semiconductor [27–29], of which band gap energy is 2.60 eV [30]. Instead, it has been shown that methylene blue in wastewater could be effectively decomposed under visible light irradiation by PbO_2 catalysts [31], of which band gap energy is 1.7 eV [32]. It appears that PbO is responsive to visible light irradiation, whereas it has been seldom applied for disposal of pollutants in wastewater. Consequently, this study devotes to assess the feasibility of mineralization of bisphenol-A in aqueous solution by PbO irradiated with visible light, wherein the influence of operating variables and inherent anions on the photocatalytic performance would be investigated, such as temperature, dosages of PbO and sulfate anions respectively. Especially, methanol, ethanol and tert-butyl alcohol individually were used as co-pollutants in the course of degradation of bisphenol-A to elucidate the presence of reactive hydroxyl radicals.

2. Experimental methods

2.1. Photocatalytic oxidation testing

The experimental system with the major apparatus involved is depicted in Fig. 1. The photocatalytic cell was a quartz cylinder equipped with a magnetic stirrer (Heidolph Corp., MR 3001K Model, Germany), wherein operation temperature was controlled through cooling coils connected with the thermostat (VWR Scientific Products Corp., 1167 Model, USA). Twelve lamps (8.6 W each) with low-pressure mercury vapor inside were used as the visible light source at the main wavelengths of 438, 550 and 619 nm (Philips Corp., PL-S Lamps, Amsterdam), which surrounded the photocatalytic cell and were sealed in a stainless box. Before tests, the wastewater feedstock (700 mL) at the bisphenol-A concentration of 100 mg/L, synthesized from deionized water and bisphenol-A (≥99%, Sigma-Aldrich, USA), was situated in the photocatalytic cell. The proportionate amounts of PbO, obtained from commercial PbO powder (≥99.9%, Alfa Aesar, USA) which was wetted and dried at 393 K for 4 h, with or without calcined at 823 K for 3 h and sieved over 400 mesh, were put into the basket located at the middle of photocatalytic cell center and wall. In this research, experiments were performed in a batch-wise mode at atmospheric pressure among the temperature range of 303–318 K. For the duration of tests, the wastewater was periodically withdrawn from the photocatalytic cell. Sequentially, the samples were undergone total organic carbon (TOC) analysis to determine residual organic compound contents. In additional experiments, four tests with different dosages of PbO (0.7 up to 1.6 g/L) were performed to explore the influence of PbO powder on the elimination of bisphenol-A. For the purpose of elucidating the effects of sulfate anions on the decomposition of bisphenol-A, a series of tests under various sodium sulfate concentrations between 0.02 and 0.10 M were carried out. In this study, all of the experimental tests were undertaken at least in duplicate to make the data reliable. The PbO would be retrieved and executed X-ray photoelectron spectroscopy (XPS) analysis after experimental tests.

2.2. TOC analysis

Within the course of photocatalytic oxidation tests, the wastewater was periodically sampled from the photocatalytic cell and directly measured utilizing a TOC analyzer (GE Corp. Sievers InnovOx), equipped with a nondispersive infrared detector. The organic ingredients in samples were completely oxidized into carbon dioxide by sodium persulfate under supercritical conditions of the water. Conversely, the inorganic ingredients, acidified by phosphoric acid, would be transformed into carbonic acid and discharged in advance. The data acquired from the TOC analyzer was corrected based on the calibration curve, which has been established among the range (0–500 mg/L) by the potassium hydrogen phthalate standard solutions.

2.3. Materials characterizations

The crystallite structures of original PbO (calcined) were determined by an X-ray diffractometer (XRD, X-MAX/2000-PC, Rigaku/SWXD, Japan) with the

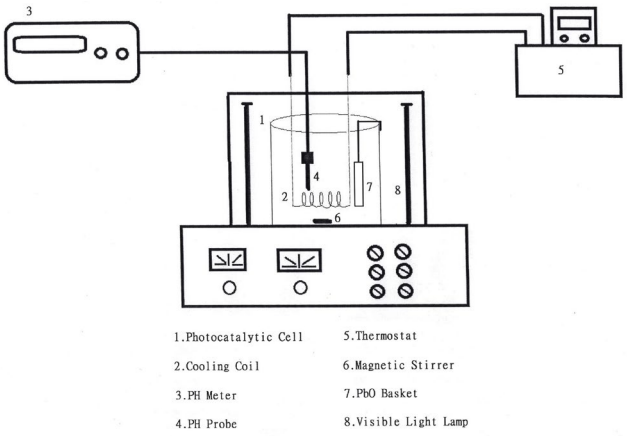

Fig. 1. Scheme of the experimental apparatus employed for photocatalytic oxidation tests.

monochromatic high-intensity CuKα radiation (λ = 1.5418 Å) under the accelerating voltage of 40 kV and emission current of 40 mA over the 2θ range of 10–80°. The Brunauer–Emmett–Teller specific surface areas of PbO (calcined) and PbO (non-calcined) were examined by the nitrogen adsorption and desorption method at 77 K using a surface area analyzing system (ASAP 2020, Micromeritics, USA). The ultraviolet-visible DRS of PbO (calcined) and PbO (non-calcined) were obtained using a UV-Vis spectrometer (UV-DRS, PerkinElmer Corp., Lambda 850 Model, USA) equipped with an integrating sphere assembly at the wavelength range of 380 to 800 nm, wherein $BaSO_4$ was used as the reference. The surface morphology of PbO (calcined) and PbO (non-calcined) was observed using a field-emission scanning electron microscope (FE-SEM, JSM-6500F, JOEL, USA). The surface electronic states of original reacted PbO (calcined) coupled with and without sodium sulfate were analyzed by an X-ray photoelectron spectrometer (XPS, Axis Ultra, Kratos analytical Ltd., UK) with a monochromatic AlKα excitation source (hν = 1486.71 eV). The binding energy scale was referenced to the C 1s core level at 284.8 eV of adventitious carbon.

2.4. Adsorption experiments

Experiments were performed in a bath-reciprocal shaker (Dong Yang Corp., DKW-40L Model, Taiwan) with a shaking speed of 100 rpm in the dark. The wastewater (250 mL) and appropriate amounts of PbO or TiO_2 powder were situated in a series of stoppered conical flasks immersed in the shaker, wherein the powder was well dispersed and operation temperature was maintained at 318 K. During the execution of adsorption tests, the conical flask was periodically withdrawn, in which the suspension solution was filtrated using syringe membrane filters (Iwaki Corp., Japan, 0.22 μm) for removal of PbO or TiO_2 powder. The clear residual wastewater was undertaken in the TOC analysis for the attainment of bisphenol-A contents.

2.5. Scavenging effects

To gain an insight into hydroxyl radicals descended from PbO semiconductors under visible light irradiation, photocatalysis of bisphenol-A was also conducted in the presence of methanol, ethanol, and tert-butyl alcohol respectively [33,34]. The samples obtained during the photocatalytic reaction were undergone UV-Vis spectrophotometry (PerkinElmer Corp., Lambda 850 Model, USA) at the wavelength of 276 nm for determination of bisphenol-A concentrations [35]. Apart from this, the difference in bisphenol-A degradation percentage between the absence of ethanol and the presence of ethanol in the photocatalytic process served as an index for the yield of hydroxyl radicals. As expected, higher yields of hydroxyl radicals (or reactive free radicals), leading to severe ethanol scavenging effect [36], would bring about a greater difference of bisphenol-A degradation percentages. Accordingly, the scavenging index would be employed for the interpretation of testing data in this work.

3. Results and discussion

3.1. Comparison of photocatalytic oxidation of bisphenol-A by PbO (calcined), PbO (non-calcined), TiO_2 (anatase) and TiO_2 (rutile)

The time-dependent patterns of TOC removal percentage using PbO (non-calcined), PbO (calcined), TiO_2 (anatase) and TiO_2 (rutile) respectively under visible light irradiation are illustrated in Fig. 2a. It clearly indicates that removal percentages of bisphenol-A via TiO_2 (anatase) and/or TiO_2 (rutile) were negligible (<8%), due to their irresponsiveness to the visible light region [37,38], whereas the obvious bisphenol-A degradation rate was obtained on PbO. It deserves to note that bisphenol-A could be mostly destructed by PbO (calcined) irradiated with visible light. The observation may be ascribed to the generation of reactive hydroxyl radicals, derived from photogenerated holes. To make clear the removal pathway of bisphenol-A, the adsorption experiments over PbO (non-calcined), PbO (calcined), TiO_2 (anatase) and TiO_2 (rutile) respectively in the dark were also carried out. The outcomes show that the amounts of bisphenol-A physically adsorbed on either PbO or TiO_2 were insignificant (referred to Fig. 2b). Thus, bisphenol-A was mainly eliminated through the photocatalytic oxidation pathway.

3.2. Optical and structural properties of PbO

UV-vis DRS of PbO (non-calcined) and PbO (calcined) are demonstrated in Fig. 3a. Both spectra of PbO exhibit the strong absorbance among the wavelength of 410 to 630 nm, which falls in the visible light region. Particularly, the spectrum of PbO (calcined) presents higher absorbance than that of PbO (non-calcined) among the wavelength of 460 to 630 nm. It seems that PbO (calcined) is more responsive to the visible light irradiation. Further, the band gap energy of PbO was estimated based on the Tauc's relation $[(\alpha h\nu)^{1/n} = A(h\nu - E_g)]$, wherein h$\nu$ is the incident photo energy, "A" is a constant and "n" is the exponent value, depending on whether the electronic transition is directly or indirectly respectively and usually takes the values 1/2 or 2, [39–41]. To find the band gap energy, the variation of $(\alpha h\nu)^2$ vs. photo energy (hν) was plotted, wherein the intercept of the tangent to the X-axis gives the band gap energy. The band gap energy of PbO (non-calcined) was determined to be 2.61 eV

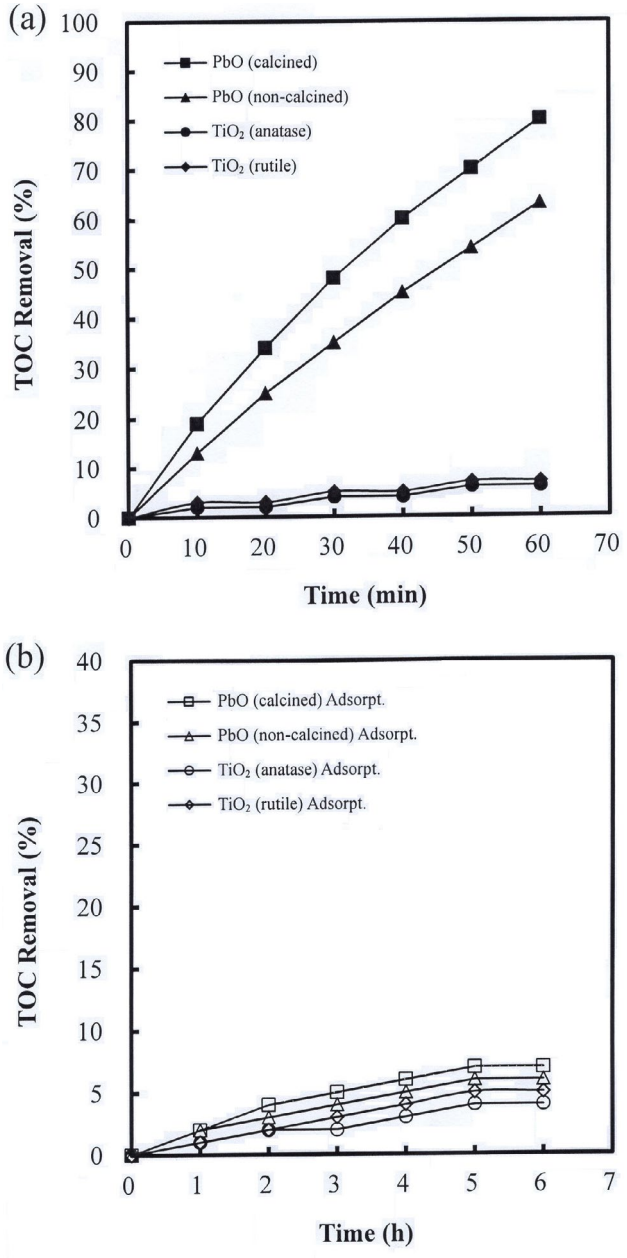

Fig. 2. (a) Time-dependent patterns of TOC removal percentage by PbO (non-calcined), PbO (calcined), TiO_2 (anatase) and TiO_2 (rutile) respectively irradiated with visible light under the conditions of visible light power = 103.2 W, T = 318 K, TiO_2 dosage = 1.0 g/L or PbO dosage = 1.0 g/L and (b) time-dependent patterns of TOC removal percentage using adsorption on the surface of PbO (non-calcined), PbO (calcined), TiO_2 (anatase) and TiO_2 (rutile) respectively under the conditions of T = 318 K, TiO_2 dosage = 1.0 g/L or PbO dosage = 1.0 g/L.

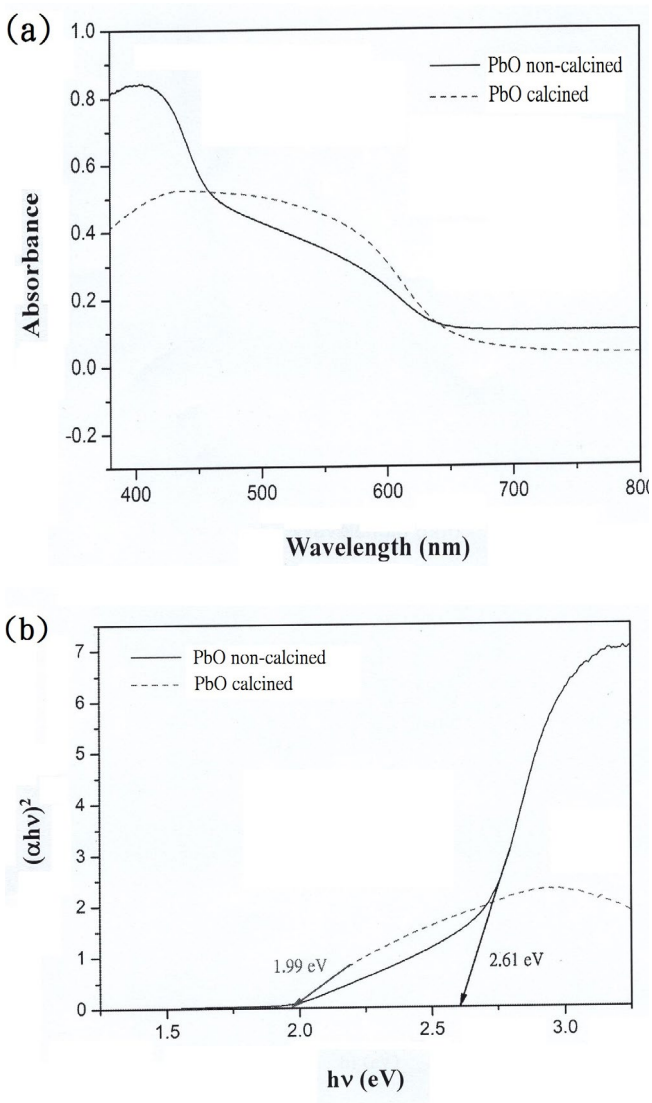

Fig. 3. (a) UV-vis DRS of PbO (non-calcined) and PbO (calcined) and (b) band gap energy of PbO (non-calcined) and PbO (calcined) was calculated based on the Tauc's relation $[(\alpha h\nu)^{1/n} = A(h\nu - E_g)]$, wherein the variation of $(\alpha h\nu)^2$ vs. photon energy ($h\nu$) was plotted.

(Fig. 3b), consistent with the literature by Suryawanshi et al. [30]. Also, the band gap energy of PbO (calcined) was evaluated to be 1.99 eV. Likewise, the specific surface area of PbO was reduced from 0.54 m^2/g (non-calcined) to 0.20 m^2/g (calcined). Due to the calcination treatment and surface morphology of PbO (calcined) smoothened (referred to Fig. 4), of which band gap energy was lower than that of PbO (non-calcined) [42–47], the superior photocatalytic behavior over PbO (calcined) may be attributed to both enhancement on charge conduction and lower band gap energy which was more sensitive to visible light.

The X-ray diffraction pattern (XRD) of the original PbO (calcined) was taken in a 2θ range from 10° to 80°, as shown in Fig. 5a. All of the reflections of the XRD pattern can be indexed to the orthorhombic lattice of α-PbO (JCPDS No. 35-1482) and the tetragonal lattice of β-PbO (JCPDS No. 01-0824) [48]. Obviously, the PbO (calcined) semiconductor is mainly composed of β-PbO of which band gap energy is 2.7 eV, whereas the minor component is α-PbO, of which

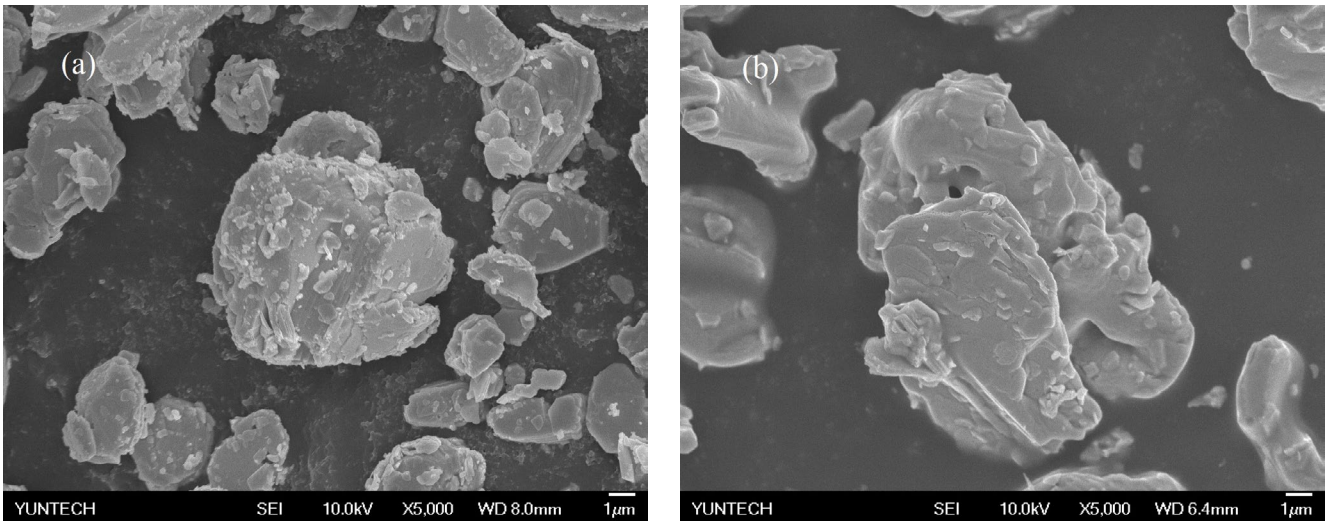

Fig. 4. FE-SEM images of the PbO semiconductors (a) PbO (non-calcined) and (b) PbO (calcined).

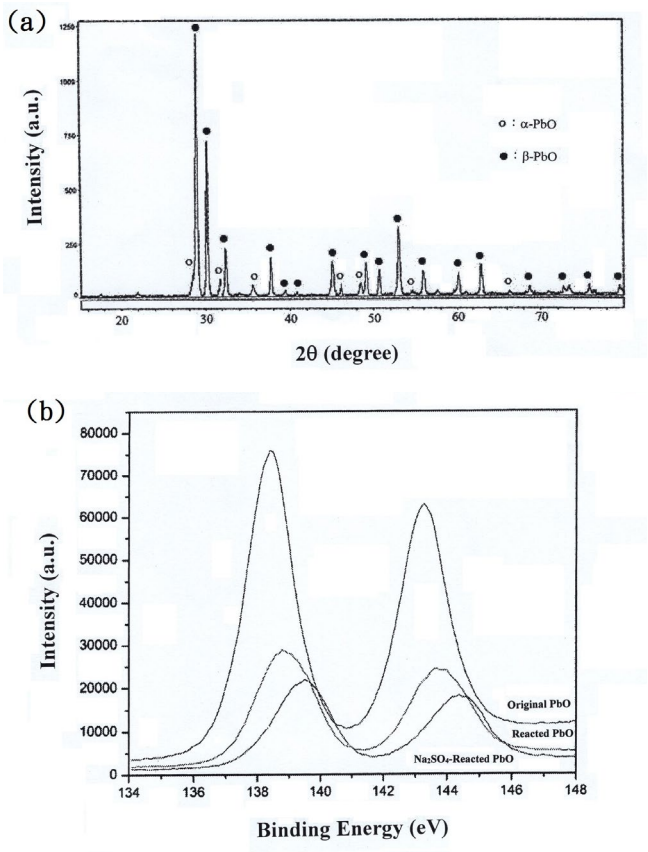

Fig. 5. (a) XRD of the original PbO (calcined) and (b) X-ray photoelectron spectra of Pb 4f core level for original PbO (calcined), reacted PbO (calcined) and reacted PbO (calcined) accompanied with sodium sulfate respectively.

band gap energy is 1.9 eV [49]. The original PbO (non-calcined) semiconductor also presents an identical XRD as that of PbO (calcined). The results agree with the band gap energy of PbO (non-calcined, 2.61 eV) as mentioned. Instead, the calcination treatment reduced the band gap energy of PbO to 1.99 eV using surface smoothness. The energy of visible light, apparently greater than the band gap of the PbO semiconductor, could excite it to generate electron-hole pairs, wherein photogenerated electrons in the conduction band may transform adsorbed oxygen into superoxide radicals and photogenerated holes in the valence band may convert adsorbed water molecules into hydroxyl radicals. Generally, the plausible reactions involved in the photocatalytic degradation of bisphenol-A using PbO can be given as follows.

$$PbO + h\nu \rightarrow h^+_{vb} + e^-_{cb} \quad (1)$$

$$BPA + h^+_{vb} \rightarrow \text{degradation products} \quad (2)$$

$$h^+_{vb} + H_2O \rightarrow H^+ + {}^{\bullet}OH \quad (3)$$

$$O_2 + e^-_{cb} \rightarrow O_2^{\bullet -} \quad (4)$$

$$O_2^{\bullet -} + 2H_2O + 2e^-_{cb} \rightarrow 3OH^- + {}^{\bullet}OH \quad (5)$$

$$BPA + {}^{\bullet}OH \rightarrow \text{degradation products} \quad (6)$$

wherein h^+_{vb} represents photogenerated holes in the valence band and e^-_{cb} represents photogenerated electrons in the conduction band.

To elucidate the surface electronic structure of PbO (calcined), XPS measurements were conducted. Fig. 5b demonstrates the Pb 4f XPS spectra of the original PbO (calcined) and reacted PbO (calcined). For original PbO (calcined), two peaks centered at 143.3 and 138.4 eV were observed, which were assigned to the binding energy of Pb $4f_{(5/2)}$ and Pb $4f_{(7/2)}$ respectively [48,50,51]. Nonetheless, after the execution of photocatalytic reaction, the binding energy of Pb $4f_{(5/2)}$ and Pb $4f_{(7/2)}$ has shifted to 143.7 and 138.8 eV

individually. It is evident that Pb cations on the surface of reacted PbO (calcined) have shifted to higher oxidation state than that of the original one, due to the migration of photogenerated electrons to the conduction band [52,53]. The results support the above hypothesis that PbO semiconductors could produce electron-hole pairs, induced by visible light irradiation. As expected, the degradation percentage of bisphenol-A by PbO was higher than that of TiO_2 in this study (referred to Fig. 2a).

3.3. Effect of dosage of scavengers on the photocatalytic oxidation of bisphenol-A by PbO (calcined)

For the insight of reactive radicals responsible for photocatalytic degradation of bisphenol-A, identical concentrations of ethanol, methanol and tert-butyl alcohol was added into the aqueous solution respectively. As illustrated in Fig. 6, the degradation percentage of bisphenol-A was significantly declined due to the introduction of ethanol or methanol, which reacted rapidly with hydroxyl radicals at the rate constants of 2.8×10^9 M^{-1} s^{-1} and 9.7×10^8 M^{-1} s^{-1} independently [33]. On the other hand, the addition of tert-butyl alcohol restrained decomposition of bisphenol-A moderately, wherein the reaction rate constant between tert-butyl alcohol and hydroxyl radicals is 6×10^8 M^{-1} s^{-1} [54,55]. The decline of bisphenol-A removal percentage corresponds to the reactivity of scavengers with hydroxyl radicals. Thus, the outcomes advocate that hydroxyl radicals, descended from photogenerated holes, were main oxidizing agents during photocatalytic oxidation of bisphenol-A.

3.4. Effect of operation temperature on the photocatalytic oxidation of bisphenol-A by PbO (calcined)

As far as photocatalytic processes are considered, it is essential to determine the appropriate operating temperature, at which the higher decomposition rate of bisphenol-A is achieved. Fig. 7 presents the time-dependent patterns of TOC removal percentage as a function of reaction temperature. It is obvious that the TOC removal rate at 318 K was higher than that at 313 K in the course of photocatalytic oxidation of bisphenol-A. Likewise, similar degradation behaviors were also observed in comparison with the data of 308 K and that of 303 K. Higher reaction temperature appears to be favorable for mineralization of bisphenol-A by PbO semiconductors. Because of suppression of oxygen solubility in aqueous solution at high temperature [56], leading to the reduction of superoxide radicals (referred to Eq.(4)), the principal oxidant for degradation of bisphenol-A could be ascribed to photogenerated holes and hydroxyl radicals derived.

3.5. Effect of PbO dosage on the photocatalytic oxidation of bisphenol-A

From the viewpoint of economics, an optimal PbO dosage for removal of bisphenol-A should be established. Fig. 8a illustrates the influence of PbO dosage on photocatalytic behaviors. It is transparent that the TOC removal percentage gave rise with increasing amounts of PbO semiconductors. In this study, bisphenol-A could be almost completely destructed under the PbO dosages of 1.6 g/L. The observation may be interpreted with an increase of PbO semiconductors irradiated by visible light, resulting in enhancement on the numbers of photogenerated holes and hydroxyl radicals. That is, the results provide evidence on our previous inference that photogenerated holes and hydroxyl radicals were main oxidizing agents. Further, to clarify the relationship between yields of hydroxyl radicals and the scavenging index, experiments with the coexistence of ethanol and bisphenol-A were performed for a variety of PbO dosages (shown in Fig. 8b). Apparently, the scavenging index indicates an identical tendency with yields of hydroxyl radicals, which reflect an analogous trend on the TOC removal percentage (operation for 60 min).

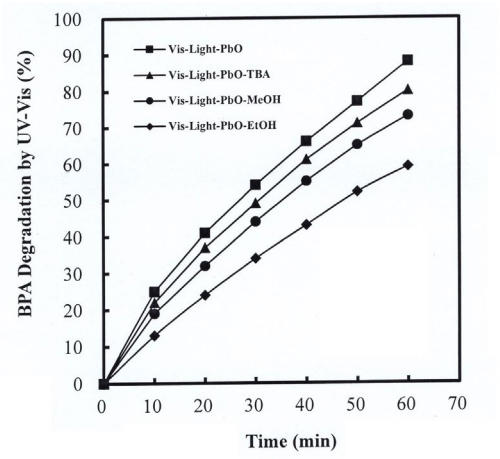

Fig. 6. Effect of coexistence of ethanol, methanol and tert-butyl alcohol respectively on the bisphenol-A degradation percentage under the conditions of visible light power = 103.2 W, T = 318 K and PbO (calcined) dosage = 1.0 g/L.

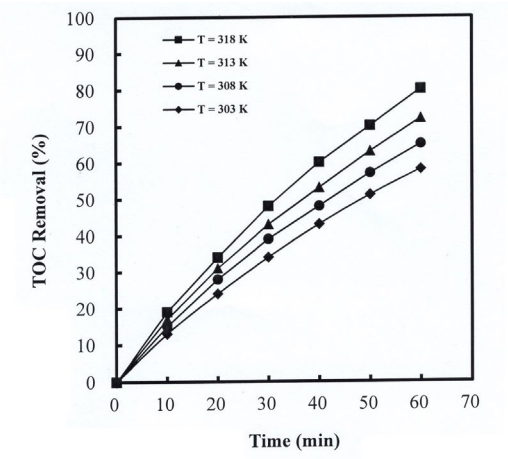

Fig. 7. Effect of operation temperature on the TOC removal percentage by PbO (calcined) irradiated with visible light under the conditions of visible light power = 103.2 W and PbO (calcined) dosage = 1.0 g/L.

3.6. Effect of sodium sulfate concentrations on the photocatalytic oxidation of bisphenol-A by PbO (calcined)

In general, sulfate anions were usually found in industrial wastewater. Consequently, it is imperative to investigate the role played by sulfate anions in this work. Fig. 9a presents the influence of sodium sulfate concentrations on the photocatalytic degradation of bisphenol-A by PbO (calcined). Transparently, the degradation percentage of bisphenol-A displays an increasing trend with sodium sulfate concentrations among the range from 0.02 to 0.10 M.

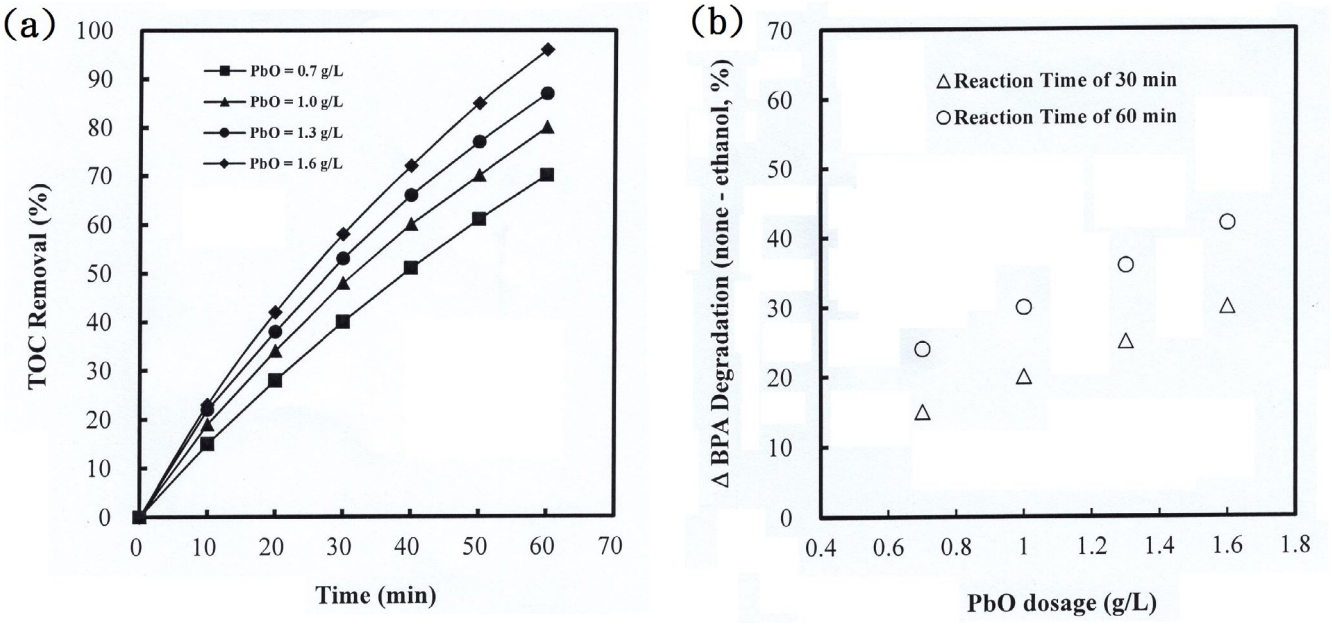

Fig. 8. (a) Effect of PbO dosages on the TOC removal percentage by PbO (calcined) irradiated with visible light under the conditions of visible light power = 103.2 W and T = 318 K. (b) The difference of bisphenol-A degradation percentage between the absence of ethanol and presence of ethanol under the conditions of visible light power = 103.2 W and T = 318 K, detected by UV-Vis spectrophotometer and served as scavenging index.

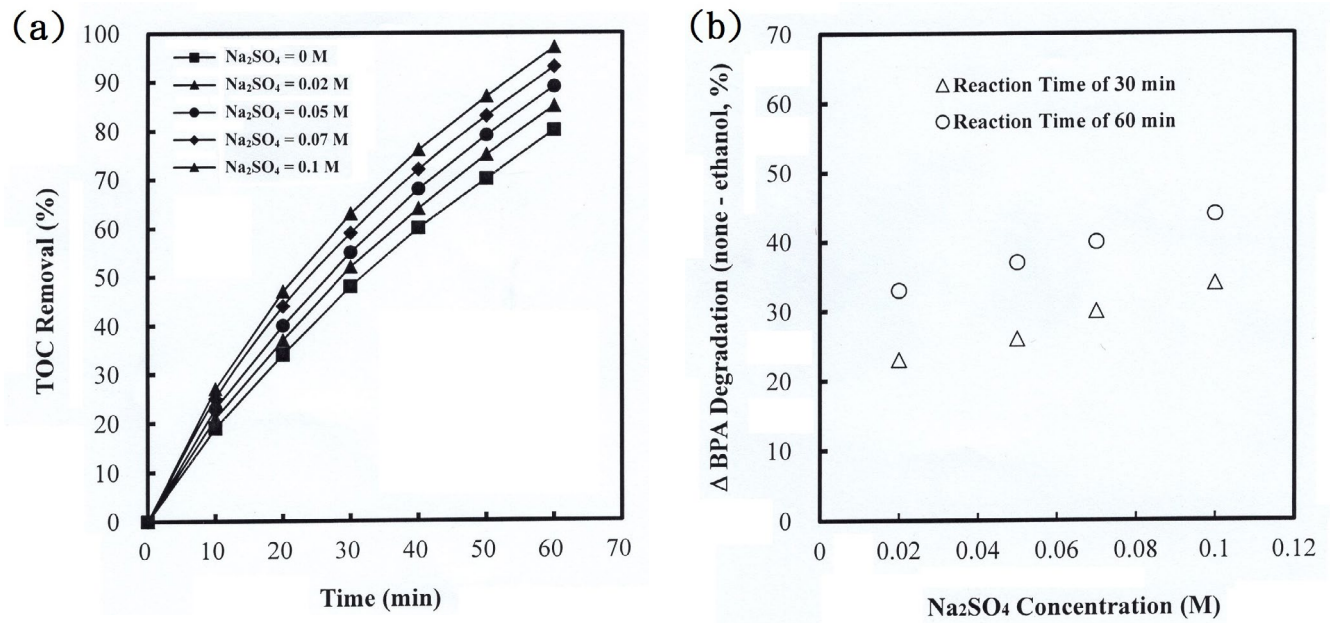

Fig. 9. (a) Effect of sodium sulfate concentrations on the TOC removal percentage by PbO (calcined) irradiated with visible light under the conditions of visible light power = 103.2 W, T = 318 K and PbO (calcined) dosage = 1.0 g/L. (b) The difference of bisphenol-A degradation percentage between the absence of ethanol and presence of ethanol under the conditions of visible light power = 103.2 W, T = 318 K and PbO (calcined) dosage = 1.0 g/L, detected by UV-Vis spectrophotometer and served as scavenging index.

It could be attributed to the generation of sulfate radicals, descended from adsorption of sulfate anions on the photogenerated holes (refer to Eq. (7)), which were simultaneously inhibited to recombine with photogenerated electrons [24,57].

$$h_{vb}^{+} + SO_4^{2-} \rightarrow SO_4^{\bullet -} \quad (7)$$

A similar trend is observed between TOC removal percentages (operation for 60 min) and scavenging index (see Fig. 9b). It reveals that except for hydroxyl radicals some sulfate radicals were also generated to promote intense ethanol scavenging effect. Thus, the introduction of sulfate anions would be beneficial for photocatalytic oxidation of bisphenol-A by PbO.

The surface electronic structure of reacted PbO (calcined) with the existence of sodium sulfate was also investigated by XPS measurements (shown in Fig. 5b). The binding energy of Pb $4f_{(5/2)}$ and Pb $4f_{(7/2)}$ has shifted to 144.4 and 139.5 eV respectively after the execution of photocatalytic reaction. That is, the Pb cations located on the surface of reacted PbO (calcined) accompanied by sulfate anions manifested a higher oxidation state than those of original and reacted PbO (calcined). The observation could be ascribed to the transformation of sulfate anions into sulfate radicals by photogenerated holes, leading to prevent recombination of photogenerated holes and electrons. In fact, the degradation percentages of bisphenol-A in the presence of both PbO (calcined) and sulfate anions were obviously higher than those of PbO (calcined) alone (refer to Fig. 9a). The results convince us of the occurrence of Eq. (7), which would make a partial contribution to the degradation of bisphenol-A.

4. Conclusions

According to the above discussion, it is apparent that bisphenol-A contaminants in aqueous solution would be chiefly decomposed by hydroxyl radicals and photogenerated holes via PbO semiconductors irradiated with visible light. Further, the removal percentage of bisphenol-A was obviously enhanced on addition of sodium sulfate, wherein sulfate anions were converted into sulfate radicals through photogenerated holes, which were prevented from recombination with photogenerated electrons. The band gap energy of PbO was significantly reduced by smoothening its surface morphology via the calcination treatment. It is noteworthy that bisphenol-A could be nearly eliminated through PbO photocatalysis. The outcomes convince us that PbO semiconductors coupled with visible light irradiation may be an economical manner for disposal of wastewater containing bisphenol-A.

References

[1] K. Weissermel, H.-J. Arpe, Industrial Organic Chemistry, Ullmann's Encyclopedia of Industrial Chemistry, VCH, Weinheim, New York, 1972, pp. 314–315.
[2] S. Flint, T. Markle, S. Thompson, E. Wallace, Bisphenol A exposure, effects, and policy: a wildlife perspective, J. Environ. Manage., 104 (2012) 19–34.
[3] J. Michałowicz, Bisphenol A - sources, toxicity and biotransformation, Environ. Toxicol. Pharmacol., 37 (2014) 738–758.
[4] Y. Zhang, W. Cui, W. An, L. Liu, Y. Liang, Y. Zhu, Combination of photoelectrocatalysis and adsorption for removal of bisphenol A over TiO_2-graphene hydrogel with a 3D network structure, Appl. Catal., B, 221 (2018) 36–46.
[5] A.O. Kondrakov, A.N. Ignatev, F.H. Frimmel, S. Bräse, H. Horn, A.L. Revelsky, Formation of genotoxic quinones during bisphenol A degradation by TiO_2 photocatalysis and UV photolysis: a comparative study, Appl. Catal., B, 160–161 (2014) 106–114.
[6] B. Erjavec, P. Hudoklin, K. Perc, T. Tišler, M.S. Dolenc, A. Pintar, Glass fiber-supported TiO_2 photocatalyst: efficient mineralization and removal of toxicity/estrogenicity of bisphenol A and its analogs, Appl. Catal., B, 183 (2016) 149–158.
[7] L. Luo, Y. Yang, M. Xiao, L. Bian, B. Yuan, Y. Liu, F. Jiang, X. Pan, A novel biotemplated synthesis of TiO_2/wood charcoal composites for synergistic removal of bisphenol A by adsorption and photocatalytic degradation, Chem. Eng. J., 262 (2015) 1275–1283.
[8] S.-D. Yoon, E.-S. Kim, Y.-H. Yun, Chemical durability and photocatalyst activity of acid-treated ceramic TiO_2 nanocomposites, J. Ind. Eng. Chem., 64 (2018) 230–236.
[9] X. Zhao, P. Du, Z. Cai, T. Wang, J. Fu, W. Liu, Photocatalysis of bisphenol A by an easy-setting titania/titanate composite: effects of water chemistry factors, degradation pathway and theoretical calculation, Environ. Pollut., 232 (2018) 580–590.
[10] K. Davididou, E. Hale, N. Lane, E. Chatzisymeon, A. Pichavant, J.-F. Hochepied, Photocatalytic treatment of saccharin and bisphenol-A in the presence of TiO_2 nanocomposites tuned by Sn(IV), Catal. Today, 287 (2017) 3–9.
[11] L.J. Luo, J. Li, J. Dai, L. Xia, C.J. Barrow, H. Wang, J. Jegatheesan, M. Yang, Bisphenol A removal on TiO_2-MoS_2-reduced graphene oxide composite by adsorption and photocatalysis, Process Saf. Environ. Prot., 112 (2017) 274–279.
[12] Z. Cheng, X. Quan, J. Xiang, Y. Huang, Y. Xu, Photocatalytic degradation of bisphenol A using an integrated system of a new gas-liquid-solid circulating fluidized bed reactor and micrometer Gd-doped TiO_2 particles, J. Environ. Sci., 24 (2012) 1317–1326.
[13] P.S. Yap, T.T. Lim, M. Lim, M. Srinivasan, Synthesis and characterization of nitrogen-doped TiO_2/AC composite for the adsorption-photocatalytic degradation of aqueous bisphenol-A using solar light, Catal. Today, 151 (2010) 8–13.
[14] P.S. Yap, T.T. Lim, Effect of aqueous matrix species on synergistic removal of bisphenol-A under solar irradiation using nitrogen-doped TiO_2/AC composite, Appl. Catal., B, 101 (2011) 709–717.
[15] X. Wang, T.T. Lim, Solvothermal synthesis of C-N codoped TiO_2 and photocatalytic evaluation for bisphenol A degradation using a visible-light irradiation LED photoreactor, Appl. Catal., B, 100 (2010) 355–364.
[16] J. Liao, W. Cui, J. Li, J. Sheng, H. Wang, X. Dong, P. Chen, G. Jiang, Z. Wang, F. Dong, Nitrogen defect structure and NO^{+} intermediate promoted photocatalytic NO removal on H_2 treated g-C_3N_4, Chem. Eng. J., 379 (2020) 122282.
[17] L.F. Chiang, R. Doong, Cu-TiO_2 nanorods with enhanced ultraviolet- and visible-light photoactivity for bisphenol A degradation, J. Hazard. Mater., 277 (2014) 84–92.
[18] C.S. Kim, J.W. Shin, Y.H. Cho, H.D. Jang, H.S. Byun, T.O. Kim, Synthesis, and characterization of Cu/N-doped mesoporous TiO_2 visible light photocatalysts, Appl. Catal., A, 455 (2013) 211–218.
[19] J. Yang, J. Dai, J. Li, Synthesis, characterization, and degradation of bisphenol A using Pr, N co-doped TiO_2 with highly visible light activity, Appl. Surf. Sci., 257 (2011) 8965–8973.
[20] X. Hao, M. Li, L. Zhang, K. Wang, C. Liu, Photocatalyst TiO_2/WO_3/GO nano-composite with a high efficient photocatalytic performance for BPA degradation under visible light and solar light illumination, J. Ind. Eng. Chem., 55 (2017) 140–148.
[21] E.B. Simsek, B. Kilic, M. Asgin, A. Akan, Graphene oxide-based heterojunction TiO_2-ZnO catalysts with an outstanding photocatalytic performance for bisphenol-A, ibuprofen and flurbiprofen, J. Ind. Eng. Chem., 59 (2018) 115–126.
[22] X. Li, W. Zhang, W. Cui, J. Li, Y. Sun, G. Jiang, H. Huang, Y. Zhang, F. Dong, Reactant activation and photocatalysis

mechanisms on Bi-metal@Bi_2GeO_5 with oxygen vacancies: a combined experimental and theoretical investigation, Chem. Eng. J., 370 (2019) 1366–1375.
[23] W. Cui, L. Chen, J. Li, Y. Zhou, Y. Sun, G. Jiang, S.C. Lee, F. Dong, Ba-vacancy induces semiconductor-like photocatalysis on insulator $BaSO_4$, Appl. Catal., B, 253 (2019) 293–299.
[24] T.B. Nguyen, C.P. Huang, R. Doong, Photocatalytic degradation of bisphenol A over a $ZnFe_2O_4/TiO_2$ nanocomposite under visible light, Sci. Total Environ., 646 (2019) 745–756.
[25] A. Iwaszuk, M. Nolan, Lead oxide-modified TiO_2 photocatalyst: tuning light absorption and charge carrier separation by lead oxidation state, Catal. Sci. Technol., 3 (2013) 2000–2008.
[26] D.S. Bhachu, S. Sathasivam, C.J. Carmalt, I.P. Parkin, PbO-modified TiO_2 thin films: a route to visible light photocatalysts, Langmuir, 30 (2014) 624–630.
[27] M. Mohammadikish, K. Zamani, Controlled construction of uniform pompon-like Pb-ICP microarchitectures as a precursor for PbO semiconductor nanoflakes, Adv. Powder Technol., 29 (2018) 2813–2821.
[28] I. Mukhopadhyay, S. Ghosh, M. Sharon, Surface modification by the potential delay technique to obtain a photoactive PbO film, Surf. Sci., 384 (1997) 234–239.
[29] D. Pavlov, Semiconductor mechanism of the processes during electrochemical oxidation of PbO to PbO_2, J. Electroanal. Chem., 118 (1981) 167–185.
[30] V.N. Suryawanshi, A.S. Varpe, M.D. Deshpande, Band gap engineering in PbO nanostructured thin films by Mn doping, Thin Solid Films, 645 (2018) 87–92.
[31] G. Li, H.Y. Yip, K.H. Wang, C. Hu, J. Qu, P.K. Wong, Photoelectrochemical degradation of methylene blue with β-PbO_2 electrodes driven by visible light irradiation, J. Environ. Sci., 23 (2011) 998–1003.
[32] W. Stumm, Chemistry of Solid-Water Interface: Processes at the Mineral-Water and Particle-Water Interface in Natural Systems, John Wiley & Sons, New York, 1992, p. 347.
[33] C.J. Liang, H.W. Su, Identification of sulfate and hydroxyl radicals in thermally activated persulfate, Ind. Eng. Chem. Res., 48 (2009) 5558–5562.
[34] H. Lin, J. Wu, H. Zhang, Degradation of bisphenol A in aqueous solution by a novel electro/ Fe^{3+}/ peroxydisulfate process, Sep. Purif. Technol., 117 (2013) 18–23.
[35] G. Zhang, Y. Xue, R. Sue, Q. Wang, W. Zhang, One-pot microwave-assisted synthesis of $Zn_{0.9}Fe_{0.1}S$ photocatalyst and its performance for the removal of bisphenol A, J. Photochem. Photobiol., A, 356 (2018) 665–672.
[36] W.S. Chen, Y.C. Shih, Mineralization of aniline in aqueous solution by sono-activated peroxydisulfate enhanced with PbO semiconductor, Chemosphere, 239 (2020) 124686.
[37] A. Bendavid, P.J. Martin, A. Jamting, H. Takikawa, Structural and optical properties of titanium oxide thin films deposited by filtered arc deposition, Thin Solid Films, 355–356 (1999) 6–11.
[38] H. Takikawa, T. Matsui, T. Sakakibara, A. Bendavid, P.J. Martin, Properties of titanium oxide film prepared by reactive cathodic vacuum arc deposition, Thin Solid Films, 348 (1999) 145–151.
[39] S.K. Maji, N. Mukherjee, A.K. Dutta, D.N. Srivastava, P. Paul, B. Karmakar, A. Mondal, B. Adhikary, Deposition of nanocrystalline CuS thin film from a single precursor: structural, optical and electrical properties, Mater. Chem. Phys., 130 (2011) 392–397.
[40] V. Štengl, T.M. Grygar, The simplest way to Iodine-doped anatase for photocatalysts activated by visible light, Int. J. Photoenergy, 2011 (2011) 685935–685948.
[41] E. Kamaraj, S. Somasundaram, K. Balasubramani, M.P. Eswaran, R. Muthuramalingam, S. Park, Facile fabrication of CuO-Pb_2O_3 nanophotocatalysts for efficient degradation of Rose Bengal dye under visible light irradiation, Appl. Surf. Sci., 433 (2018) 206–212.
[42] Y.R. Denny, T. Firmansyah, Isnaeni, S. Aritonang, A.M. Kartina, Evaluation of band gap energy and surface roughness for tin indium zinc oxide thin films by atomic force microscopy and electron spectroscopy, IOP Conf. Ser.: Mater. Sci. Eng., 343 (2018) 012006.
[43] M. Singh, A. Yadav, S. Kumar, P. Agarwal, Annealing induced electrical conduction and band gap variation in thermally reduced graphene oxide films with different sp^2/sp^3 fraction, Appl. Surf. Sci., 326 (2015) 236–242.
[44] H. Huang, S. Tu, C. Zeng, T. Zhang, A.H. Reshak, Y. Zhang, Macroscopic polarization enhancement promoting photo- and piezoelectric-induced charge separation and molecular oxygen activation, Angew. Chem. Int. Ed., 56 (2017) 11860–11864.
[45] F. Chen, H. Huang, L. Guo, Y. Zhang, The role of polarization in photocatalysis, Angew. Chem. Int. Ed., 58 (2019) 10061–10073.
[46] L. Hao, L. Kang, H. Huang, L. Ye, K. Han, S. Yang, H. Yu, M. Batmunkh, Y. Zhang, T. Ma, Surface-halogenation-induced atomic-site activation and local charge separation for superb CO_2 photoreduction, Adv. Mater., 31 (2019) 1900546.
[47] F. Chen, H. Huang, L. Ye, T. Zhang, Y. Zhang, X. Han, T. Ma, Thickness-dependent facet junction control of layered $BiOIO_3$ single crystals for highly efficient CO_2 photoreduction, Adv. Funct. Mater., 28 (2018) 1804284.
[48] M. Salavati-Niasari, F. Mohandes, F. Davar, Preparation of PbO nanocrystals via decomposition of lead oxalate, Polyhedron, 28 (2009) 2263–2267.
[49] L.M. Droessler, H.E. Assender, A.A.R. Watt, Thermally deposited lead oxides for thin-film photovoltaics, Mater. Lett., 71 (2012) 51–53.
[50] Y.-C. Lai, J.-C. Lin, C. Lee, Nucleation and growth of highly oriented lead titanate thin-films prepared by a sol-gel method, Appl. Surf. Sci., 125 (1998) 51–57.
[51] F.-Y. Liu, J.-H. Lin, Y.-M. Dai, L.-W. Chen, S.-T. Huang, T.-W. Yeh, J.-L. Chang, C.-C. Chen, Preparation of perovskites $PbBiO_2I$/PbO exhibiting visible-light photocatalytic activity, Catal. Today, 314 (2018) 28–41.
[52] C.-H. Park, M.-S. Won, Y.-H. Oh, Y.-G. Son, An XPS study and electrical properties of $Pb_{1.1}Zr_{0.53}Ti_{0.47}O_3$/PbO/Si (MFIS) structures according to the substrate temperature of the PbO buffer layer, Appl. Surf. Sci., 252 (2005) 1988–1997.
[53] D.A. Zatsepin, D.W. Boukhvalov, N.V. Gavrilov, A.F. Zatsepin, V.Ya. Shur, A.A. Esin, S.S. Kim, E.Z. Kurmaev, Soft electronic structure modulation of surface (thin-film) and bulk (ceramics) morphologies of TiO_2-host by Pb-implantation: XPS-and-DFT characterization, Appl. Surf. Sci., 400 (2017) 110–117.
[54] P. Neta, R.E. Huie, A.B. Ross, Rate constants for reactions of inorganic radicals in aqueous solution, J. Phys. Chem. Ref. Data, 17 (1988) 1027–1284.
[55] G.V. Buxton, C.L. Greenstock, W.P. Helman, A.B. Ross, Critical review of rate constants for reactions of hydrated electrons, hydrogen atoms and hydroxyl radicals ($^{\bullet}OH/^{\bullet}O^-$) in aqueous solution, J. Phys. Chem. Ref. Data, 17 (1988) 513–886.
[56] D. Tromans, Temperature and pressure-dependent solubility of oxygen in water: a thermodynamic analysis, Hydrometallurgy, 48 (1998) 327–342.
[57] J.F. Gomes, A. Lopes, M. Gmurek, R.M. Quinta-Ferreira, R.C. Martins, Study of the influence of the matrix characteristics over the photocatalytic ozonation of parabens using Ag-TiO_2, Sci. Total Environ., 646 (2019) 1468–1477.